

SCOUR ANALYSIS DOWNSTREAM OF PAUTE-CARDENILLO DAM

LUIS G. CASTILLO⁽¹⁾, JOSÉ M. CARRILLO⁽²⁾

⁽¹⁾ *Hidr@m Group, Universidad Politécnica de Cartagena, Cartagena, Spain, luis.castillo@upct.es*

⁽²⁾ *Hidr@m Group, Universidad Politécnica de Cartagena, Cartagena, Spain, jose.carrillo@upct.es*

Abstract

The study analyzes the expected changes in the Paute River, located in Ecuador, as a result of the construction of the Paute-Cardenillo Dam. To evaluate the stability and safety of the structure, it is necessary to ascertain the shape and dimensions of the scour generated downstream. The scour is studied with three complementary procedures: empirical formulae obtained in models and prototypes, semi-empirical methodology based on pressure fluctuations-erodibility index and computational fluid dynamics (CFD) simulations. A pre-excavated stilling basin is proposed and analyzed.

Keywords: CFD; Dam safety; Erodibility; Scour; Semi-empirical methodology

1. Dam Characteristics

The Paute-Cardenillo Dam (owned by Celec Ep-Hidropaute), located in Ecuador, is a double curvature arch dam with a maximum height of 135 m to the foundations. The top level is located at an altitude of 926 meters. The reservoir has a length of 2.98 km with normal maximum water level located at 924 meters. The dam will integrate the National Electric System of Ecuador with a total electricity installed capacity of 600 MW which will produce 13000 GWh per year.

It has a half-height outlet with two almost symmetrical ducts. Considering the maximum normal operating level (924 m), the intermediate outlet capacity is $Q_{40} = 1760 \text{ m}^3/\text{s}$. The half-height outlet, operating together with the free surface weir, achieves a capacity of $Q_{100} = 2340 \text{ m}^3/\text{s}$. If the bottom outlet were considered, the discharge capacity of the dam would be $Q_{10000} = 5520 \text{ m}^3/\text{s}$.

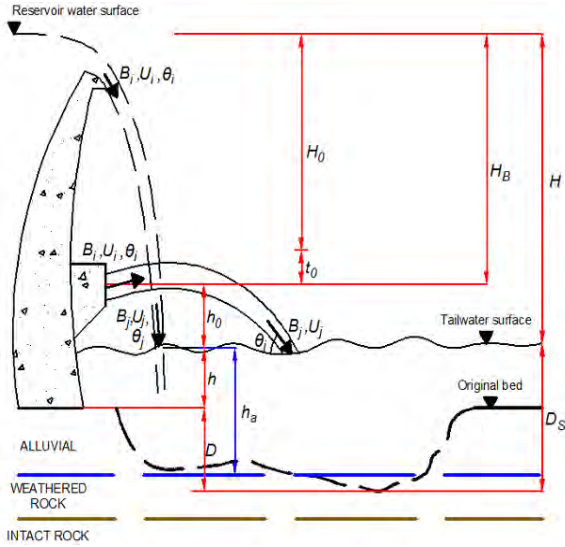
2. Empirical formulae

In the study, 29 formulae are examined for flows of various return periods.

Most of the equations were obtained by dimensional and statistic analysis of data obtained in Froude scale reduced models, with few formulae based on prototypes and many obtained for the ski-jump. As discharge is produced by a free surface weir and in pressure conditions by an half-height outlet, the general expression is modified which provides the following simplified general expression:

$$D_s = h + D = K \frac{q^x H_n^y h^w}{g^v d^z} \quad [1]$$

where D_s is the scour depth below tailwater level, h the tailwater depth, D the scour depth below the original bed, K an experimental coefficient, q the specific flow, H_n the energy net head, and d the characteristic size of bed material. The meaning of the rest variables can be seen in Figure 1.



x, y, w, v, z . Empirical exponents defined by regression or optimization.
 t_0 = energy losses in the duct.
 $H_n = H_0 = H_B - t_0$. Net energy head at the exit of the outlet.
 $H_n = H$. Falling height from reservoir level to tailwater level (ski-jump and free surface weir).
 h_0 . Vertical distance between outlet exit and tailwater level.
 h_a . Vertical distance between tailwater level and alluvial scour.
 B_i, U_i, θ_i . Thickness, velocity and angle of the jet in initial conditions.
 B_j, U_j, θ_j . Total thickness, velocity and angle of the jet in impingement conditions.

Figure 1. Scheme of scour in Paute-Cardenillo Dam.

Table 1 shows the coefficients corresponding to five simplified formulae with values that fall in the mean values ± 1 standard deviation, while Table 2 shows five more general expressions with values in the same range.

Figure 2 shows the results obtained for the half-height outlet. The mean value ± 1 standard deviation is indicated. The jet would scour the alluvial layer (24 m) with a return period flow $Q_{22} = 1320 \text{ m}^3/\text{s}$. The design flow ($Q_{40} = 1760 \text{ m}^3/\text{s}$) would not reach the intact rock. However, if the mean value $+ 1$ standard deviation were taken into account, then the flow of $1250 \text{ m}^3/\text{s}$ would erode the weathered rock layer (scour about 34 m).

Table 1. Coefficients of five scour simplified formulae with values that fall in the mean value ± 1 standard deviation.

Author	K	x	y	z	d
Schoklitsch, 1932	0.521	0.57	0.20	0.32	d_{90}
Damle-C, 1966	0.362	0.50	0.50	0	-
Martins-B, 1975	1.500	0.60	0.10	0	-
Tairamovich, 1978	0.633	0.67	0.25	0	-
Suprassi, 2007	0.150	0.38	0.75	0	-

Table 2. Five scour general formulae with values that fall in the mean value +/- 1 standard deviation.

AUTHOR (YEAR)	FORMULAE
Jaeger (1939)	$D_s = 0.6q^{0.5}H_n^{0.25}(h/d_m)^{0.333}$
Mirskhulava (1967)	$D_s = \left(\frac{0.97}{\sqrt{d_{90}}} - \frac{1.35}{\sqrt{H_n}} \right) \frac{q \cdot \sin\theta_T}{1 - 0.175 \cdot \cot\theta_T} + 0.25h$
Mason-B (1989)	$D_s = 3.39 \frac{q^{0.60}(1 + \beta)^{0.30}h^{0.16}}{g^{0.30}d_m^{0.06}}$
Modified Veronese (1994)	$D_s = 1.90h^{0.225}q^{0.54} \cdot \sin\theta_T$
Bombardelli and Gioia (2006)	$D_s = K \frac{q^{0.67}H_n^{0.67}h^{0.15}}{g^{0.33}d_{90}^{0.33}} \left(\frac{\rho}{\rho_s - \rho} \right)$

d_m . Average particle size of the bed material.
 d_{90} . Bed material size in which 90% is smaller in weight.
 θ_T . Impingement jet angle.
 g (9.81 m/s²). Gravity.
 β . Air-water relationship.
 ρ . Water density.
 ρ_s . Density of sediment.

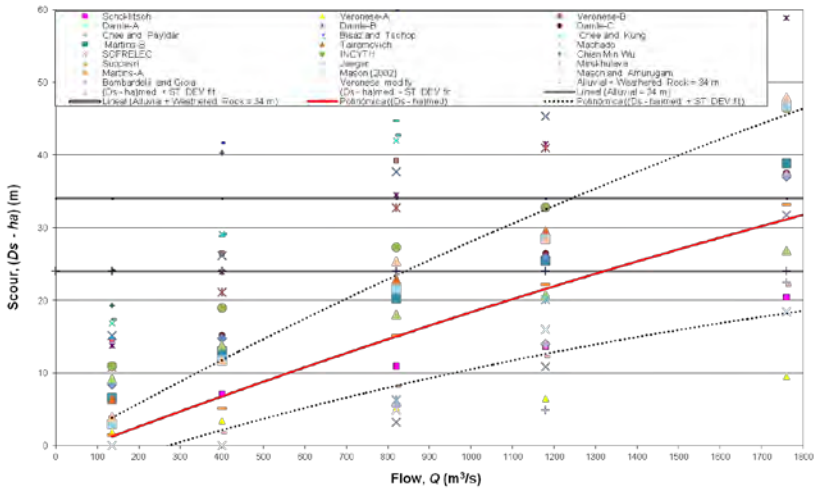


Figure 2. Scour of alluvial and weathered rock for the half-height outlet.

3. Semi-empirical methodology

The erodibility index is based on an erosive threshold that relates the magnitude of relative erosion capacity of water and the relative capacity of a material (natural or artificial) to resisting scour. There is a correlation between the stream power or magnitude of the erosive capacity of water (P) and a mathematical function [$f(K)$] that represents the relative capacity of the material to resisting erosion. On the erosion threshold, this may be expressed by the relationship $P = f(K)$. If $P > f(K)$, with the erosion threshold being exceeded and the material eroded.

Scour in turbulent flow is not a shear process. It is caused by turbulent, fluctuating pressures (Annandale, 2006). Quantification of pressure fluctuations of incident jets in stilling basins has been studied mainly by Ervine and Falvey, 1987; Ervine *et al.*, 1997; Castillo, 1989, 2002, 2006,

2007; Castillo *et al.*, 1991, 2007; Puertas, 1994; Bollaert, 2002; Bollaert and Schleiss, 2003; Melo *et al.*, 2006; and Felderspiel, 2011.

The dynamic pressures of jets are a function of the turbulence intensity at the discharge conditions, length of the jet flight, diameter (circular jet) or thickness (rectangular jet) in impingement jet conditions and water cushion depth.

Annandale, 1995, 2006, summarized and established a relationship between the stream power and the erodibility index for a wide variety of materials and flow conditions. The stream power per unit of area available of an impingement jet is:

$$P_{jet} = \frac{\gamma QH}{A} \quad [2]$$

where γ is the specific weight of water, Q the flow, H the drop height or the upstream energy head, and A the jet area on the impact surface. The erodibility index is defined as:

$$K = M_s \cdot K_b \cdot K_d \cdot J_s \quad [3]$$

where M_s is the mass strength number, K_b the block or particle size number, K_d the discontinuity bond shear strength number, and J_s the relative ground structure number. Table 3 shows the formulae of the parameters.

Table 3. Erodibility index parameters (Adapted from Annandale, 2006).

Material	Formulae	Parameters
Rock	$M_s = 0.78C_r UCS^{1.05}$ when $UCS \leq 10 \text{ MPa}$ $M_s = C_r UCS$ when $UCS > 10 \text{ MPa}$ $C_r = \frac{\rho_r}{\gamma_r}$	UCS . Unconfined compressive strength. C_r . Coefficient of relative density. ρ_r . Mass density of the rock. g (9.81 m/s ²). Gravity. γ_r (27 · 10 ³ N/m ³). Reference unit weight of rock.
Non-cohesive granular soil	The relative magnitude is obtained by means of the standard penetration test (<i>SPT</i>). When the <i>SPT</i> value exceeds 80, the non-cohesive granular material is taken as rock.	
Rock	$K_b = \frac{RQD}{J_n}$	RQD values range between 5 and 100, J_n between 1 and 5, and K_b between 1 and 100. RQD . Rock quality designation. J_n . Joint set number.
Non-cohesive granular soil	$K_b = 1000D^3$	D . Characteristic particle diameter.
Rock	$K_d = \frac{J_r}{J_a}$	J_r . Joint wall roughness number. J_a . Joint wall alteration number.
Non-cohesive granular soil	$K_d = \tan\phi$	ϕ . Residual friction angle of the granular earth material.

The threshold of rock strength to the stream power, expressed in kW/m², is calculated and based on the erodibility index K :

$$P_{rock} = 0.48K^{0.44} \quad \text{if} \quad K \leq 0.1 \quad [4]$$

$$P_{rock} = K^{0.75} \quad \text{if} \quad K > 0.1 \quad [5]$$

The dynamic pressure in the bottom of the stilling basin is based on two components: the mean dynamic pressure (C_p) and the fluctuating dynamic pressure ($C_p \hat{\gamma}$). These dynamic pressure coefficients are used as estimators of the stream power reduction coefficients, by an effect of

the jet disintegration in the air and their diffusion in the stilling basin (Annandale, 2006). Hence, the dynamic pressures are also a function of the fall height to disintegration height ratio (H/L_b) and water cushion to impingement jet thickness (Y/B_j). Thus, the total dynamic pressure is expressed as:

$$P_{total} = C_p(Y/B_j)P_{jet} + FC_p'(Y/B_j)P_{jet} \quad [6]$$

where $C_p(Y/B_j)$ is the mean dynamic pressure coefficient, $C_p'(Y/B_j)$ the fluctuating dynamic pressure coefficient, P_{jet} the stream power per unit of area, and F the reduction factor of the fluctuating dynamic pressure coefficient.

We can observe that the analyzed case does not correspond strictly with circular neither rectangular (nappe flow) jet case. For circular jets, the C_p and C_p' are valid for $H/L_b \leq 0.50$ (Ervine et al., 1997). However, for the design flow ($Q_{40} = 1760 \text{ m}^3/\text{s}$) the $H/L_b = 1.67$. For rectangular jet case, Castillo and Carrillo, 2012, 2013, adjusted the formulae by using new laboratory data (Figures 3, 4 and 5), valid for a wide H/L_b ratio.

For this reason the calculus were carried out by using the rectangular analogy. Tables 4 and 5 show the values of the different variables considered and their respective calculus in the semi-empirical methodology.

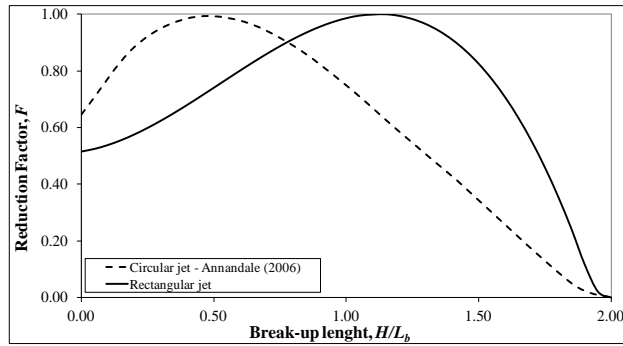


Figure 3. Reduction factor F of fluctuating dynamic pressure coefficient.

Table 4. Semi-empirical methodology. Intact rock input and calculated values.

Angle of rock friction, SPT ($^{\circ}$)	38	Number of join system (calculated), J_n	1.83
Specific weight (KN/m^3)	27.64	Discontinuity spacing, J_x, J_y, J_z (m)	0.50
Unconfined compress. resistant, UCS (Mpa)	50	Average block diameter (calculated), (m)	0.50
Relative density coefficient, C_r	1.024	Roughness degree, J_r	2
RQD (calculated)	90	Alteration degree, J_a	1

Table 5. Semi-empirical methodology. Concrete input and calculated values.

Specific weight (KN/m^3)	27.64	Number of join system (calculated), J_n	1.50
Unconfined compress. resistant, UCS (Mpa)	20	Discontinuity spacing, J_x, J_y, J_z (m)	0.01
Relative density coefficient, C_r	1.024	Average block diameter (calculated), (m)	0.50
RQD (calculated)	100	Roughness degree, J_r	4
		Alteration degree, J_a	0.75

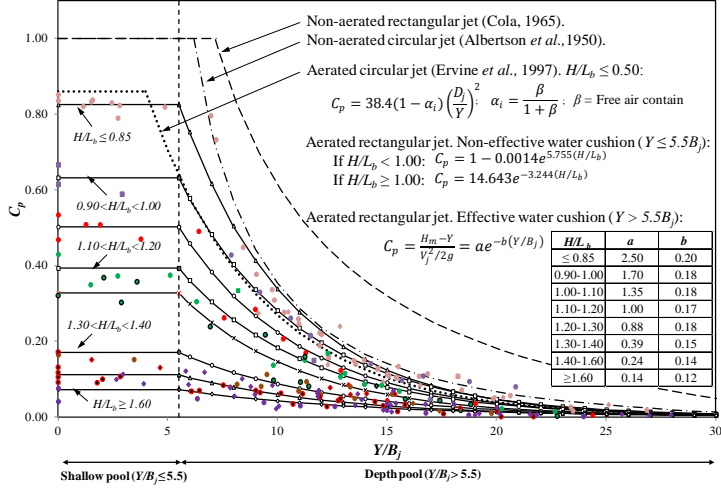


Figure 4. Mean dynamic pressure coefficient, C_p , for the aerated circular and rectangular jet.

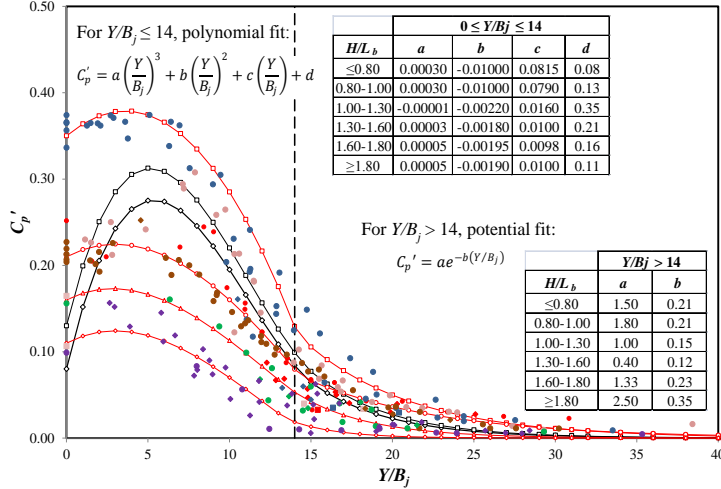


Figure 5. Fluctuant dynamic pressure coefficient, C_p' , for the rectangular jet.

Considering a water cushion of 26 m (bed scour $D = 24$ m), the stream power threshold of weathered rock ($P_{weathered_rock} = 15.92$ kW/m²) does not resist the flow of annual return period ($Q_{ma} = 136$ m³/s). The intact rock stream power ($P_{rock} = 407.46$ kW/m²) could resist up to a flow return period of 5 years ($Q_5 = 820$ m³/s). The $Q_{10} = 1180$ m³/s would exceed the rock strength.

A concrete slab of 20 MPa characteristic strength and thickness of 2 m ($P_{conc} = 788$ kW/m²) is placed directly on the alluvial level (796 m). The geometry of the pre-excavated basin should be similar to the geometry of the basin that would be formed with the flow $Q_{40} = 1760$ m³/s. Figure 6 indicates that the concrete slab would resist the power stream of the design flow ($P_{jet} = 664.95$ kW/m²).

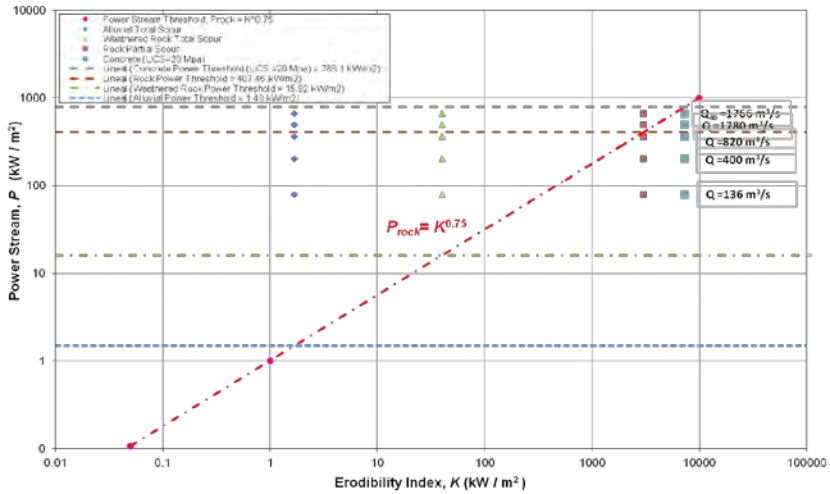


Figure 6. Half-height outlet. Stream power of the jet for different flows as a function of the erodibility: intact rock and concrete cases ($D_s = 24$ m).

Table 6 shows the principal parameters and the results obtained in the intact rock and the concrete slab proposed for the pre-excavated stilling basin.

Table 6. Parameters, Erodibility index and Stream power ($D_s = 24$ m). Intact rock and Concrete cases.

	Intact rock	Concrete
M_s	51.19	20.47
K_b	49.18	66.67
K_d	2.00	5.33
J_s	0.60	1.00
Erodibility index, K	3020.77	7279.67
Stream power, $P_{material}$ (kw/m ²)	407.46	788.10

4. Numerical simulation

As a complement of the empirical and semi-empirical methodologies, three-dimensional mathematical model simulations were carried out. These programs allow a more detailed characterization than one-dimensional and two-dimensional numerical models and, thus, a detailed study of local effects of the sediments transport. The numerical simulation of the hydraulic behavior and scour by the action of the free surface weir, intermediate and bottom outlets were also analyzed.

The computational fluid dynamics (CFD) program FLOW-3D was used. This program solves the Navier-Stokes equations discretized by finite differences. It incorporates various turbulence models, a sediment transport model and an empirical model bed erosion (Guo, 2002; Mastbergen and Von den Berg, 2003; Brethour and Burnham, 2011), together with the VOF method for calculating the free surface of the fluid without solving the air component (Hirt and Nichols, 1981).

In order to calibrate the CFD simulations, sensibility analysis was carried out. The mesh size, the turbulent model and his correspondent Turbulent Mixing Length ($TLEN$) were analyzed. For the selection of the mesh size, the dimensions of the half-height outlet ducts (5.00×5.80 m) and the thickness of the falling jets were considered. The mesh consisted in hexahedral elements of 1 m. The Re-Normalization Group (RNG) $k-\epsilon$ turbulence model was selected. The volume-of-fluid advection was solved with the Split Lagrangian method. The time-step size was controlled by stability and convergence criteria.

Pressures obtained in the stagnation point and their associated mean dynamic pressure coefficients were compared with the parametric methodology proposed by Castillo (2006, 2007).

As far as the numerical simulation is concerned, the scour shape considering the concrete slab was analyzed. In this way, the level 798 m was considered as a non erodible.

For the design flow, the half-height outlet jets tend to impact on a small area. The upstream face of the scour occurred approximately 85 m downstream from the dam. The plant scour was near 108 m long and 50 m wide (Figure 7). Scour would reach the left natural slope and could cause landslides. The pre-excavated stilling basin shape should be adjusted to the geometry and the space available. Figure 8 shows the velocities vectors in lateral and top views of the pre-excavated basin.

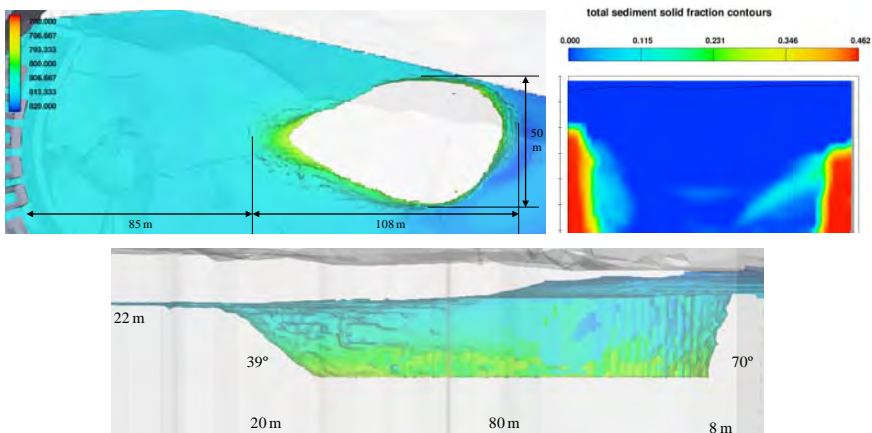


Figure 7. Top, front and lateral views of the scour due to the half-height outlet.

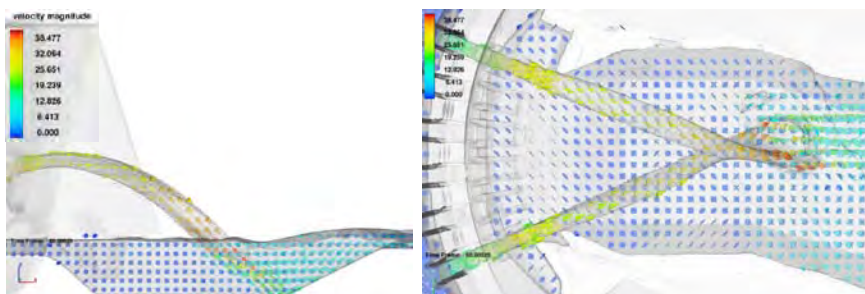


Figure 8. Lateral and top views of the velocity vectors in the pre-excavated stilling basin.

5. Conclusions

In this paper, similar results have been obtained by solving the problem from three different complementary perspectives: empirical formulations, erosion potential semi-empirical formulation and CFD simulations. The results demonstrate the suitability of crossing methodologies to solve complex phenomena. Thus, numerical simulations were used to complement the classical formulations and semi-empirical methodology, allowing a better understanding of the physical phenomena in order to obtain an adequate solution.

Methodology leads us to propose a pre-excavated stilling basin. The basin would allow to generate an effective water cushion. Besides this, it would reduce the sedimentation due to the excavation and the material transported by the river, especially during the flushing operations of the reservoir. The pre-excavated basin also would help to have a symmetric and regular flow, reducing the risk of potential landslides.

Acknowledgments

The authors are grateful to CELEC EP - Hidropaute and the Consorcio POYRY-Caminosca Asociados for the data provided.

References

- Albertson, M. L., Dai, Y. B., Jenson, R. A. and Rouse, H. 1950. 'Diffusion of Submerged Jets', Proceedings ASCE.
- Annandale, G. W. 1995. 'Erodibility', Journal of Hydraulic Research, 33 (4), 471-494.
- Annandale, G.W. 2006. 'Scour Technology. Mechanics and Engineering Practice', McGraw-Hill.
- Bollaert, E. 2002. 'Transient Water Pressures in Joint and Formations of Rock Scour due to High-Velocity Jet Impact, Communication N°. 13', Laboratory of Hydraulic Constructions, École Polytechnique Fédérale de Lausanne, Switzerland.
- Bollaert, E.F., and Schleiss, A. 2003. 'Scour of rock due to the impact of plunging high velocity jets. Part 1: A state-of-the-art review', Journal of Hydraulic Research, 41(5), 451-464.
- Bombardelli, F.A., Gioia, G. 2006. 'Scouring of granular beds by jet-driven axisymmetric turbulent cauldrons', Phys. Fluids 18(8), 088101.
- Brethour, J., and Burnham, J. 2010. 'Modeling Sediment Erosion and Deposition with the FLOW-3D Sedimentation & Scour Model', Flow Science Tech. Note, FSI-10-TN85, 1-22.
- Castillo, L. 1989. 'Metodología experimental y numérica para la caracterización del campo de presiones en los disipadores de energía hidráulica. Aplicación al vertido en presas bóveda', PhD Thesis, Universitat Politècnica de Catalunya, Barcelona, Spain (in Spanish).
- Castillo, L. (2002). 'Parametrical Analysis of the Ultimate Scour and Mean Dynamic Pressures at Plunge Pools', Workshop on Rock Scour due to High Velocity Jets, École Polytechnique Fédérale de Lausanne.
- Castillo, L. 2006. 'Areated jets and pressure fluctuation in plunge pools', The 7th International Conference on Hydrosience and Engineering (ICHE-2006), IAHR, ASCE, Drexel University. College of Engineering, DU Haggerty Library, Philadelphia, USA.

- Castillo, L., Puertas, J. and Dolz, J. 2007. 'Discussion about Scour of rock due to the impact of plunging high velocity jets Part I: A state-of-the-art review', *Journal of Hydraulic Research*, 45 (6), 853-858.
- Castillo, L. (2007). 'Pressure characterization of undeveloped and developed jets in shallow and deep pool', 32nd Congress of IAHR, the International Association of Hydraulic Engineering & Research, Vol.2, 645-655, Venice, Italy.
- Castillo, L.G., and Carrillo, J.M. 2012. 'Hydrodynamics characterization in plunge pool. Simulation with CFD methodology and validation with experimental measurements', 2nd IAHR Europe Congress, Munich.
- Castillo, L.G., and Carrillo, J.M. 2013. 'Analysis of the ratio scale in nappe flow case by means of CFD numerical simulations', *Proceedings of 2013 IAHR Congress*, Chengdu, China.
- Cola, R. 1965. 'Energy dissipation of a high-velocity vertical jet entering a basin', *Proceedings of the 11th Congress of the IAHR*, Leningrad.
- CONSORCIO PCA 2012. 'FASE B: Informe de Factibilidad, Anexo 2, Meteorología, Hidrología y Sedimentología'.
- CONSORCIO PCA 2012. 'FASE B: Informe de Factibilidad, Anexo 6, Hidráulica'.
- Ervine, D. A., and Falvey, H.R. 1987. 'Behavior of turbulent jets in the atmosphere and plunge pools', *Proceedings of the Institutions of Civil Engineers*, 83 (2), 295-314.
- Ervine, D. A., Falvey, H.R. and Whithers, W. 1997. 'Pressure Fluctuations on Plunge Pool Floors', *Journal of Hydraulic Research*, 35 (2).
- Felderspiel, M.P. 2011. 'Response of an embedded block impacted by high-velocity jets', PhD Thesis, École Polytechnique Fédérale de Lausanne, Suisse.
- Flow Sciences Incorporated. 2011. 'FLOW-3D Users Manual Version 10.0', Santa Fe, New Mexico.
- Hirt, C. W., and Nichols, B. D. 1981. 'Volume of Fluid (VOF) Method for the Dynamics of Free Boundaries', *Journal of Computational Physics*, 39 (201).
- Guo, J. (2002). 'Hunter Rouse and Shields diagram', *Proc 1th IAHR-APD Congress*, Singapore, 2, 1069-1098.
- Martins, R., 1975. 'Scouring of rocky riverbeds by free-jet spillways', *Water Power & Dam Construction*, April, 1975.
- Mason, P.J. and Arumugan, K. 1985. 'Free Jets Scour below Dams and Flip Buckets', *Journal of Hydraulic Engineering*, ASCE, 111(2), 220-235.
- Mason, P.J. 1989. 'Effects of air entrainment on plunge pool scour', *Journal of Hydraulic Engineering*, ASCE, 115(3), 385-399.
- Mastbergen, D. R. and Von den Berg J. H. 2003. 'Breaching in fine sands and the generation of sustained turbidity currents in submarine canyons', *Sedimentology*, 50, 625-637.
- Melo, J. F., Pinheiro, A. N., and Ramos, C. M. 2006. 'Forces on plunge pool slabs: influence of joints location and width', *Journal of Hydraulic Engineering*, 132 (1), 49-60.
- Puertas, J. 1994. 'Criterios hidráulicos para el diseño de cuencos de disipación de energía en presas bóveda con vertido libre por coronación', PhD Thesis, Universidad Politécnica de Cataluña, Spain (in Spanish).
- Suppasri, A. 2007. 'Hydraulic performance of Nam Ngum 2 spillway', *Asian Institute of Technology: Pathumthni*.
- Taraimovich, I. I. 1978. 'Deformation of channels below high head spillways on rock foundations', *Hydrotechnical Construction*, 9, 917-922.